Biosensors and Bioelectronics 78 (2016) 213–220

Contents lists available at ScienceDirect

Biosensors and Bioelectronics

journal homepage: www.elsevier.com/locate/bios

Detecting trypsin at liquid crystal/aqueous interface by using surface-immobilized bovine serum albumin

Cheng-Hao Chuang [a], Yi-Cheng Lin [b], Wei-Long Chen [b], Yu-Hsuan Chen [b], Yu-Xun Chen [a], Chieh-Ming Chen [a], Hung Wei Shiu [c], Lo-Yueh Chang [c], Chia-Hao Chen [c], Chih-Hsin Chen [b,*]

[a] Department of Physics, Tamkang University, New Taipei City 25137, Taiwan
[b] Department of Chemistry, Tamkang University, New Taipei City 25137, Taiwan
[c] National Synchrotron Radiation Research Center, Hsinchu 30076, Taiwan

ARTICLE INFO

Article history:
Received 24 September 2015
Received in revised form
9 November 2015
Accepted 15 November 2015
Available online 17 November 2015

Keywords:
Liquid crystal-based biosensor
Bovine serum albumin
Trypsin
Scanning photoelectron microscopy

ABSTRACT

We report a new mechanism for liquid crystal (LC)-based sensor system for trypsin detection. In this system, bovine serum albumin (BSA) was immobilized on gold grids as the enzymatic substrate. When the BSA-modified grid was filled with LC and immersed in the solution containing trypsin, the peptide bonds of BSA were hydrolyzed and peptide fragments were desorbed from the surface of gold grid, which disrupted the orientation of LC at the vicinity and resulted in a dark-to-bright transition of optical image of LCs. By using this mechanism, the limit of detection (LOD) of trypsin is 10 ng/mL, and it does not respond to thrombin and pepsin. Besides, the cleavage behavior on gold surfaces was directly visualized by the scanning photoelectron microscopy (SPEM), in particular for the chemical composition identification and element-resolved image. The loss of BSA fragments and the enhancement of Au photoelectron signal after trypsin cleavage were corresponding to the proposed mechanism of the LC-based sensor system. Because the signals reported by LC can be simply interpreted through the human naked-eye, it provides a simple method for fast-screening trypsin activity in aqueous solution.

1. Introduction

Trypsin is a digestive enzyme produced in the pancreas. It maintains the function of human digestive system by hydrolyzing the proteins into smaller peptide fragments, which is easier to transport into the small intestine and utilized in cellular metabolism. In addition, it is also responsible for other physiological functions such as immune response and blood coagulation. Loss of trypsin activity can lead to serious conditions such as cystic fibrosis (Noone et al., 2001). Therefore, the development of analytical system which can precisely detect trypsin with high sensitivity is critically needed. To detect trypsin, most of current approaches applied a peptide-immobilized surface as substrate and the specific cleavage events occurred on the surface can be reported by different signals such as fluorescence (Fan et al., 2012; Suzuki et al., 2008), electrochemistry (Abd-Rabboh et al., 2003; Dong et al., 2015) and surface-enhanced Raman scattering (Chen et al., 2013) with high sensitivity. However, these techniques require expensive instrumentation and trained technicians for data processing such that limit their applicability.

Alternatively, liquid crystal (LC)-based sensors have been considered as a cheaper and simpler approach for biological sensing applications. The key advantage of using LC-based system is the pre-labeling of the targets is not required, and the sensing read outs are colorful thus can be identified by naked-eye. By studying the interfacial phenomenon involving the orientation of LC, LC-based sensors have been used to detect various targets of interest such as DNA (Chen and Yang, 2010), proteins (Gupta et al., 1998), bacteria (Sivakumar et al., 2009), viruses (Han et al., 2014), glucose (Kim et al., 2013), organophosphates (Chen and Yang, 2013), bile acids (Bera and Fang, 2013), protons (Bi et al., 2009), and heavy metal ions (Yang et al., 2013). In previous studies, the principles to detect the enzyme at the LC/aqueous interface by using the LC-based sensors can be classified into two types. One of them applied enzymatic substrates which are pre-added in the aqueous phase. The reorientation of LC is caused by the hydrolytic products produced from the specific enzymatic reaction occurred in the aqueous phase. For example, Hu et al. developed the LC-based sensor to monitor urease activity in aqueous solution through the hydrolysis of urea by urease to produce ammonia (Hu and Jang, 2011). The presence of ammonia increases the pH of solution that can be reported by LC-based pH sensor as bright-to-dark transition of its optical signals. Besides, they also developed the LC-based sensor to monitor lipase activity in aqueous solution through the

* Corresponding author.
E-mail address: chc@mail.tku.edu.tw (C.-H. Chen).

http://dx.doi.org/10.1016/j.bios.2015.11.049
0956-5663/

hydrolysis of glyceryl trioleate to produce oleic acids (Hu and Jang, 2012). The presence of oleic acids simultaneously forms a self-assembled monolayer (SAM) at the LC/aqueous interface which blocks the LC from contacting the aqueous phase and leads to bright-to-dark transition of optical images of the LC. However, the results of this system are pH-dependent as it relies on the deprotonation of aliphatic acids to form amphiphilic molecules in order to align the LC at interface. The other type for LC-based enzyme sensor is designed by directly applying a layer of enzymatic substrate at the LC/aqueous interface to block the LC from contacting the aqueous phase. The reorientation of LC is derived from the enzymatic hydrolysis of substrates which allows the LC to contact with aqueous phase. For instance, Hussain et al. applied a monolayer of phospholipids at an LC/aqueous interface to monitor lipase activity (Hussain et al., 2014). In addition, Zhang et al. applied a poly-L-lysine-based polymeric membrane at an LC/aqueous interface to monitor trypsin activity (Zhang and Jang, 2013). In this type of the LC-based sensors, the optical identification is correlated to the ideal immobilization of the monolayer of substrate at the LC/aqueous interface. Because the precise characterization of such monolayer at the interface is challenging, the performance of this type of sensor is not optimal.

Bovine serum albumin (BSA) is a globular protein produced in cows. Because it is chemically stable and does not interfere with biological reactions, it is commonly used as the blocking agent for immunoassays or the stabilizing agent for enzyme storage. Recently, several studies demonstrated that BSA can also act as the enzyme substrate for trypsin detection. For example, Hu et al. applied BSA-stabilized gold nanoclusters as the fluorescence probe to detect trypsin. The addition of trypsin hydrolyzed BSA into amino acids or peptide fragments and therefore lowered the fluorescence intensity of gold nanoclusters, allowing the sensitive detection of trypsin at 0.01 μg/mL (Hu et al., 2012). On the other hand, Yazgan et al. reported that BSA can be used as the substrate to bind with Raman reporter molecules, creating the signal of surface-enhanced Raman scattering (SERS) on solid surface. The enzymatic hydrolysis on BSA lowered the intensity of SERS such that the activity of enzyme was quantified (Yazgan et al., 2010). As a substrate of enzyme, the structure, stability, and orientation of BSA immobilized on solid surfaces have been studied previously. To the best of our knowledge, there is no study focusing on characterizing the interface influenced by the hydrolysis of surface-immobilized BSA. Although an enhanced vibration signal in SERS technology is strongly affected by certain target metals, molecular bonding groups, as well as nanoparticle hybrid substrates (Yazgan et al., 2010), it is not an optimal platform to identify the effect of enzymatic hydrolysis on the chemical nature of complex BSA network immobilized on the surface.

In this study, the LC-based sensor system utilizing a BSA-modified gold grid for trypsin detection is reported for the first time. Previous studies have demonstrated that the orientation of LC at the LC/aqueous interface can be controlled by applying amphiphilic molecules such as surfactants (Brake and Abbott, 2002), polyelectrolytes (Lee et al., 2010) and lipids (Brake et al., 2003) at the interface. We proposed that after BSA is hydrolyzed by trypsin, peptide fragments will be released from the surface of gold grid to the vicinity of LC, leading to the reorientation of LCs as well as a differentiable change in the LC texture. To further investigate the change in the composition of surface-immobilized BSA before and after trypsin hydrolysis, X-ray photoelectron spectroscopy (XPS) was applied to characterize the element-sensitive surface density and chemical bonding of BSA under various conditions. For space-resolved information, we offered a novel imaginable approach with the surface and element sensitivity to characterize the trypsin activity directly by scanning photoelectron microscopy (SPEM) (Chuang et al., 2007).

2. Materials and methods

2.1. Materials

Glass slides were obtained from Fisher Scientific (U.S.A). *N,N*-Dimethyl-*n*-octadecyl-3-aminopropyltrimethoxysilyl chloride (DMOAP), sodium cyanoborohydride ($NaBH_3CN$), 50% glutaraldehyde aqueous solution (GA), bovine serum albumin (BSA), fluorescein isothiocyanate isomer I (FITC), trypsin, pepsin and were purchased from Sigma Aldrich (U.S.A). Tris buffer was purchased from J.T. Baker (U.S.A). Liquid crystal 4-cyano-4′-pentylbiphenyl (5CB) was purchased from TCI (Taiwan). 4′-n-decyloxybiphenyl-4-carboxylic acid (DCA) was synthesized following reported procedures (Coco et al., 2000). Water was purified by using a Milli-Q system (Millipore).

2.2. Preparation of DMOAP-coated slides

To clean the surface, glass slides were immersed in a 5% Decon-90 solution (a commercially available detergent) for 2 h, sonicated in deionized water for 15 min, and rinsed thoroughly with deionized water twice. After this, the slides were dried under a stream of nitrogen. The cleaned glass slides were immersed in an aqueous solution containing 0.1% (v/v) DMOAP for 5 min, and then rinsed with copious amounts of deionized water. DMOAP-coated slides were dried under a stream of nitrogen and heated in a 100 °C vacuum oven for 15 min.

2.3. Immobilization of BSA on gold grid

TEM gold grids (75, 100, 200, and 400 mesh, Ted Pella, Inc., U.S.A) were cleaned in methanol, ethanol, and acetone (sonicated in each solvent for 15 min), and then heated overnight at 100 °C to evaporate residual solvent. To immobilize BSA on the surface, the clean grids were immersed in PBS buffer containing BSA (1 mg/mL) for 30 min then rinsed with deionized water. Next, the grids were immersed in an aqueous solution containing BSA (1 mg/mL), glutaraldehyde (5 wt%) and sodium cyanoborohydride (10 mM) under constant shaking for 16 h. After that, the grids were washed thoroughly with deionized water to remove non-specifically adsorbed BSA.

2.4. Preparation of LC samples

The DMOAP-coated glass slides were cut into squares (5 mm × 5 mm) for supporting LC. Then, a BSA-modified grid was placed on the slide, and approximately 0.3 μL of 5CB doped with 0.3 wt% of 4′-n-decyloxybiphenyl-4-carboxylic acid (DCA) was dispensed onto the grid. Excessive LC was removed by using a capillary tube. Finally, the grid containing the LC was immersed in 200 μL of Tris buffer (100 mM, pH = 8.4) containing different concentrations of trypsin. The effect of the pH value of solution on the LC images of the system was shown in Fig. S1. For the stability of the system, we set the pH value of solution at 8.4 because it can maintain the dark LC images for more than 12 h. The optical appearances of these samples were observed by using a polarizing optical microscope (Canon EOS D650, Japan) in the transmission mode. Each image was captured with a digital camera mounted on the microscope with an exposure time of 1/80 sec.

2.5. XPS measurements

To study the surface properties by XPS, the 1000 mesh gold grid (mesh size ~20 μm) was immersed into the 1 mg/mL of BSA and 100 ng/mL of trypsin solution sequentially, controlled by the combined CCD and XYZ positioning system. The BSA/gold sample

with/without trypsin was measured by XPS in the beamline 09A1 at National Synchrotron Radiation Research Center (NSRRC), Taiwan. A highly energy resolution (< 0.2 eV) and incident photon energy (380.0 eV) used in SPEM are calibrated by the Au 4f states of Au foil (Chuang et al., 2007).

3. Results and discussion

3.1. Effect of surface-immobilized BSA on the optical image of LCs at the LC/aqueous interface

In order to understand how the surface-immobilized BSA affects the optical images of LC at the LC/aqueous interface, we placed the BSA-modified grids on a DMOAP-coated slide and filled them with the LCs (5CB) doped with 0.3 wt% of 4′-n-decyloxybiphenyl-4-carboxylic acid (DCA). DCA is an amphiphilic molecule composed of a hydrophobic hydrocarbon chain and a pH-sensitive functional group (-COOH). In previous studies, this type of molecules has been applied at the LC/aqueous interface to control the orientation of LC (Bi et al., 2009; Chen et al., 2015). Fig. 1a shows that when the whole system was immersed into the buffer solution, the optical image of LC is mostly dark inside the square region. Such dark image can be attributed to the formation of a layer of deprotonated DCA at the LC/aqueous interface, which functions as amphiphiles to align LCs homeotropically at the LC/aqueous interface. However, when we inspect the LC image of the periphery of the square region in more detail, we found that some of the LC appears bright at the vicinity of gold grid, and the shape of bright LC region is irregular. In contrast, when a bare grid was

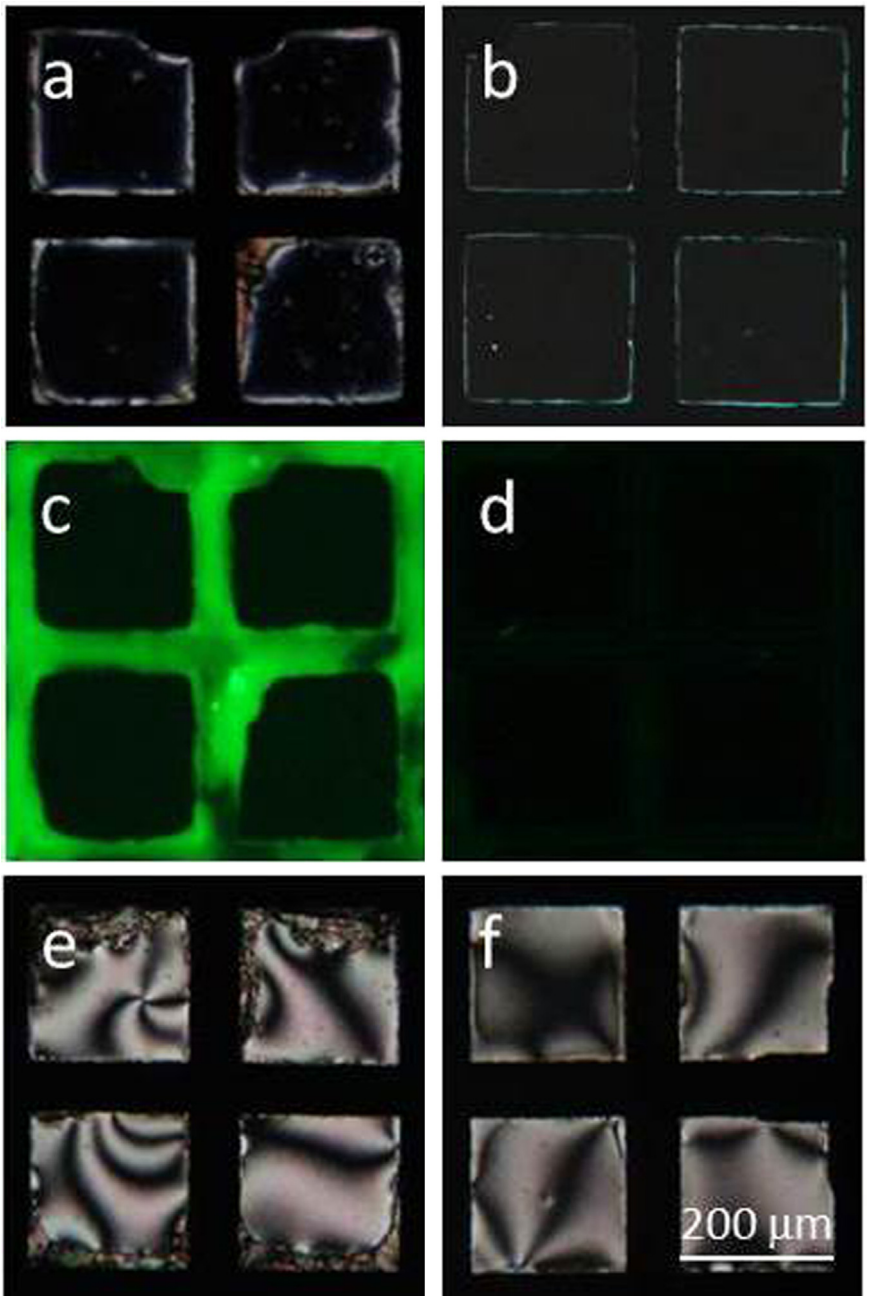

Fig. 1. Polarized images of (a) BSA-modified grids hosting 4′-n-decyloxybiphenyl-4-carboxylic acid doped 5CB, (b) bare grids hosting 4′-n-decyloxybiphenyl-4-carboxylic acid doped 5CB. (c) and (d) are the respective fluorescence images of the grids in (a) and (b) after FITC-labeling the BSA on the grid. (e) BSA-modified grids hosting pure 5CB and (f) bare grids hosting pure 5CB immersed in Tris buffer (100 mM, pH=8.4).

used under the same conditions (Fig. 1b), the LC inside the square region is remains dark without irregular shape of bright LC at the vicinity of gold grid. In this case, only a very thin layer of LC turned bright at the vicinity of gold grid due to the boundary effect. To confirm that BSA was immobilized on grid, we further immersed both BSA-modified grid and bare grid in a solution containing FITC-labeling regent. After rinsing with deionized water, the grids were observed under fluorescence microscope. It was found that BSA-modified grid is strongly fluorescent after labeling (Fig. 1c); while no fluorescence was observed on the bare grid (Fig. 1d). Therefore, we can conclude that the irregular bright LC image at the vicinity of gold grid is caused by the presence of surface-immobilized BSA nearby LC, which disrupted the orientation of LC from homeotropic to planar. On the other hand, we also carried out two additional control experiments by using BSA-modified grid and bare grid filled with 5CB without doping DCA. Fig. 1e and f show that the LC images are bright when 5CB was used only. For a better contrast of signals in the LC-based sensor, we selected the LC doped with DCA in the following studies.

3.2. Effect of mesh size of grid on the optical image of LCs at the LC/aqueous interface

The mesh size of grid determines the number LC molecules confined in a specific square region, which is a potential factor to affect the orientation of LC. For this reason, we immobilized BSA on 75, 100, 200 and 400 mesh grids to investigate the optical images of LC in these grids. The results show that LC image was dark when the grid is 75 and 100 mesh (Fig. 2a and b), while LC image became bright when the grid is 200 and 400 mesh (Fig. 2c and d). When we further looked into the fluorescence image after the grids were labeled with FITC tag, it was found that BSA was immobilized on the grids regardless of the mesh size. These results suggest that the effect of immobilized BSA on the orientation of LC depends on the mesh size of grid. The width of the square for 75, 100, 200, and 400 mesh grids are 284 μm, 204 μm, 90 μm, and 38 μm, respectively. From previous studies, we knew that LC molecules are able to communicate their orientations in the vicinity region up to 100 μm (Xue and Yang, 2008). Therefore, the bright LC image in 200 and 400 mesh grids can be explained by the long-range communication between LC molecules and the immobilized BSA on the grid. For the dark background of the LC-based sensor system, we used 100 mesh grids in the following experiments.

3.3. Detection of trypsin by using BSA-modified gold grids as substrate

Among the 607 amino acids of BSA, there are 60 lysine and 26 arginine residues that can be hydrolyzed by trypsin. Hence, our next goal was to study whether the enzymatic reaction of trypsin can be reported by the optical images of LC by using BSA-modified gold grids as the substrate. Fig. 3a shows that after we immersed the system into a solution containing 100 ng/mL of trypsin for 10 min, the LC image, which was originally dark, turned bright. In contrast, when the system was immersed into a solution without trypsin, most the LC image in the square region was still dark (Fig. 3b). By examining the mass spectra of the aqueous solution after the LC image turned bright, we also found the presence of peptide fragments of which the molecular weight is less than 1215 (Fig. S2). Therefore, the dark-to-bright transition of LC image is possibly due to that cleaved peptide fragments desorbed from the surface of grid and disrupted the orientation of LC inside the grid (Scheme 1). Besides, we also noticed that the texture of the bright LC image in our system is similar to that demonstrated by the formation of oligopeptide-based polymeric membranes at the LC/aqueous interface in previous study (Park et al., 2006), which indicates a tilted or parallel orientation of LC at interface after the LC contacted with oligopeptide. To further confirm this point, we immersed the system using bare grids into a solution containing 100 ng/mL of trypsin. It was found that the LC image was dark in the solution containing trypsin only (Fig. 3c), which implies that trypsin along was not able to lead the reorientation of LC. Based on these observations, we conclude that the trypsin in aqueous phase can be detected through the dark-to-bright transition of the LC image at the LC/aqueous interface. To examine the specificity of this system, we immersed the system into a buffer solution containing 100 ng/mL of thrombin and pepsin, respectively. The

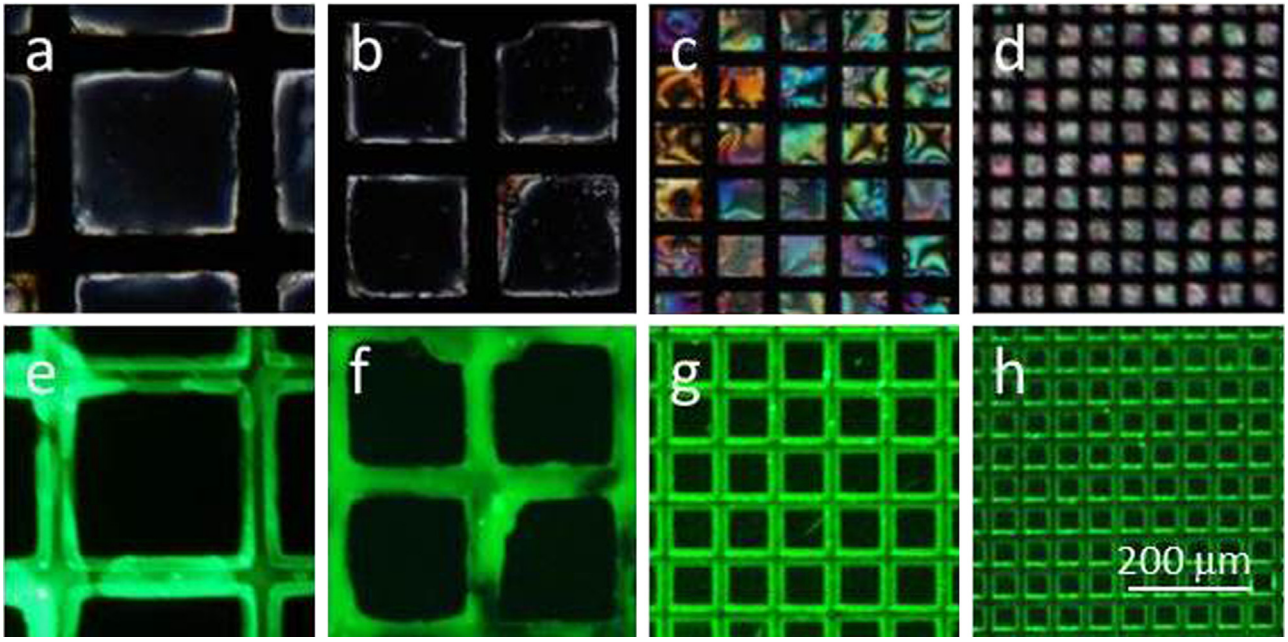

Fig. 2. Polarized image of (a) 75 mesh, (b) 100 mesh, (c) 200 mesh and (d) 400 mesh BSA-modified grids hosting 4′-n-decyloxybiphenyl-4-carboxylic acid doped 5CB immersed in Tri buffer (100 mM, pH = 8.4). (e) to (d) are the fluorescence image of the grid in (a) to (d) after FITC-labeling the BSA on the grid. These results indicated that the LC image is dark only when the grid is smaller than 100 mesh.

Fig. 3. Polarized image of BSA-modified grids hosting 4′-n-decyloxybiphenyl-4-carboxylic acid doped 5CB immersed in (a) 100 ng/mL trypsin, (b) Tris buffer, (c) 100 ng/mL trypsin (bare grids were used instead of BSA-modified grids), (d) 100 ng/mL thrombin, (e) 100 ng/mL pepsin. It shows that trypsin can be detected through the dark-to-bright transition of LC image when BSA-modified grids were used.

results show that the LC images in the square region were dark (Fig. 3d and e), which means the optical response of this system is specific to trypsin. It does not response to thrombin, which has no cleavage sites on BSA, and pepsin, which has the working pH range from 1.5 to 3.5. To determine the limit of detection (LOD) of the reported system, we compared the optical images of the LCs at different concentrations of trypsin. Fig. 4 shows that LC image turned bright when the concentration of trypsin is higher than 10 ng/mL, while it remained dark when the concentration of trypsin is lower than 1 ng/mL. By plotting a graph of the mean brightness value of the LC images against the logarithm of trypsin concentration, we noticed that there is a sharp increase in brightness when the trypsin concentration increased from 1 ng/mL to 10 ng/mL (Fig. S3). As a result, we determined that the LOD for trypsin by using this system is approximately 10 ng/mL.

3.4. Characterization of trypsin cleavage on surface-immobilized BSA by using SPEM

To investigate how the trypsin hydrolyzes the BSA immobilized on gold surface, the BSA areas with/without trypsin immersion on the same piece of gold grid were utilized for the comprehensive comparison. The in-depth probing for the chemical images of the grids, BSA, and trypsin-immersed BSA was visualized by the micro-XPS analysis. Fig. 5a and c are the grid images collected at C 1s and Au $4f_{7/2}$ state photoelectrons at binding energy (BE) of 285.2 eV and 84.1 eV, where can be easily recognized as the boundary region between bare and BSA-modified grids. The insets of Fig. 5a and c show the high-magnified images to amplify the chemical contrast on the 0th (bare), 1st (BSA), and boundary (white dot-lines). The intensity line profiles (right panel of Fig. 5a and c) acquired from the A–B line demonstrated that when BSA was immobilized on the top of gold grid, C 1s signal in 1st range is larger than that in 0th range. On the other hand, the signal of Au photoelectrons from the bottom gold grids was blocked by the top layer such that the intensity of Au $4f_{7/2}$ signal in 1st range became one-fourth of that in 0th range. The boundary area showed the intensity fluctuation of C 1s signal due to lower concentration and disordered assemblage of BSA on the edge of gold/BSA, and in consequence the Au signal became the lowest too. In fact, the edge effect observed at the boundary area is also corresponding to the irregular bright LCs at the vicinity of the surface-immobilized BSA grid in Fig. 1a. The XPS spectra at different positions (1, 2, and 3; marked in the inset of Fig. 5a and c), reflect the chemical environments of BSA and Au grid indicative of 0th, boundary, and 1st area, after the background subtraction and signal normalization. In Fig. 5b, a carbon contamination layer is unavoidable to be detected on the surface of Au grid (position 1) due to the ambient environment and high surface-sensitivity of XPS, constituted of hydrocarbon group (C–H) at BE of 284.5 eV (Azioune et al., 2005; Frateur et al., 2007). At position 3, different amino acids, typical of C–C chain (285.2 eV), C–N/C–S groups (286.4 eV), and C=O–O/C=N–O groups (288.0 eV), are known to raise higher BE side of C 1s state (Rubio et al., 2002; Chevrier et al., 2012). The chemical shift and intensity contrast of C 1s state make the position-dependent BSA surface spatially resolvable. Hence, in Fig. 5d, gold grids at position 1 have much intensive signal in Au $4f_{5/2}$ (87.7 eV) and $4f_{7/2}$ (84.1 eV) states comparing with that at position 2 and 3,

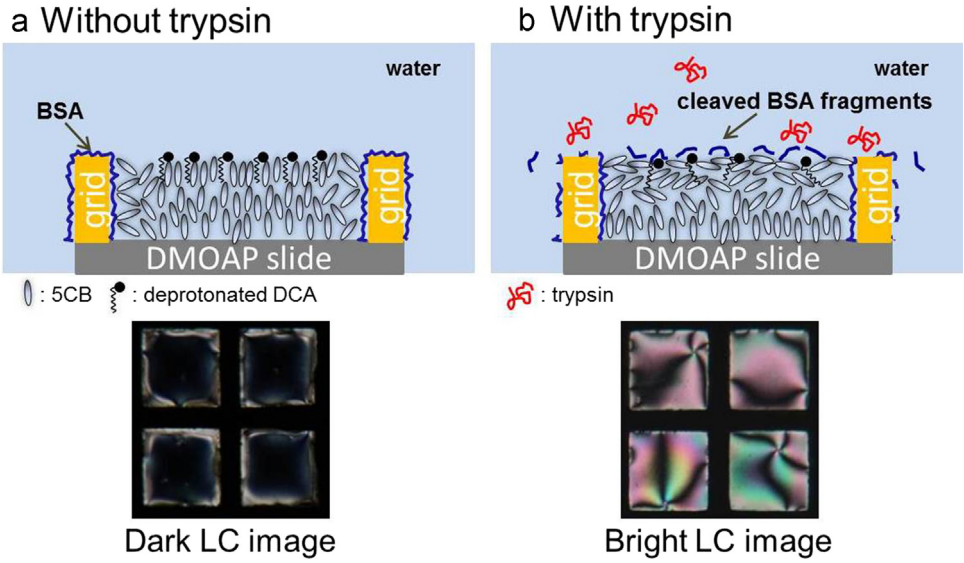

Scheme 1. Schematic illustration of the LC orientation and corresponding images for the LC-based sensor system (a) without and (b) with trypsin in the aqueous solution.

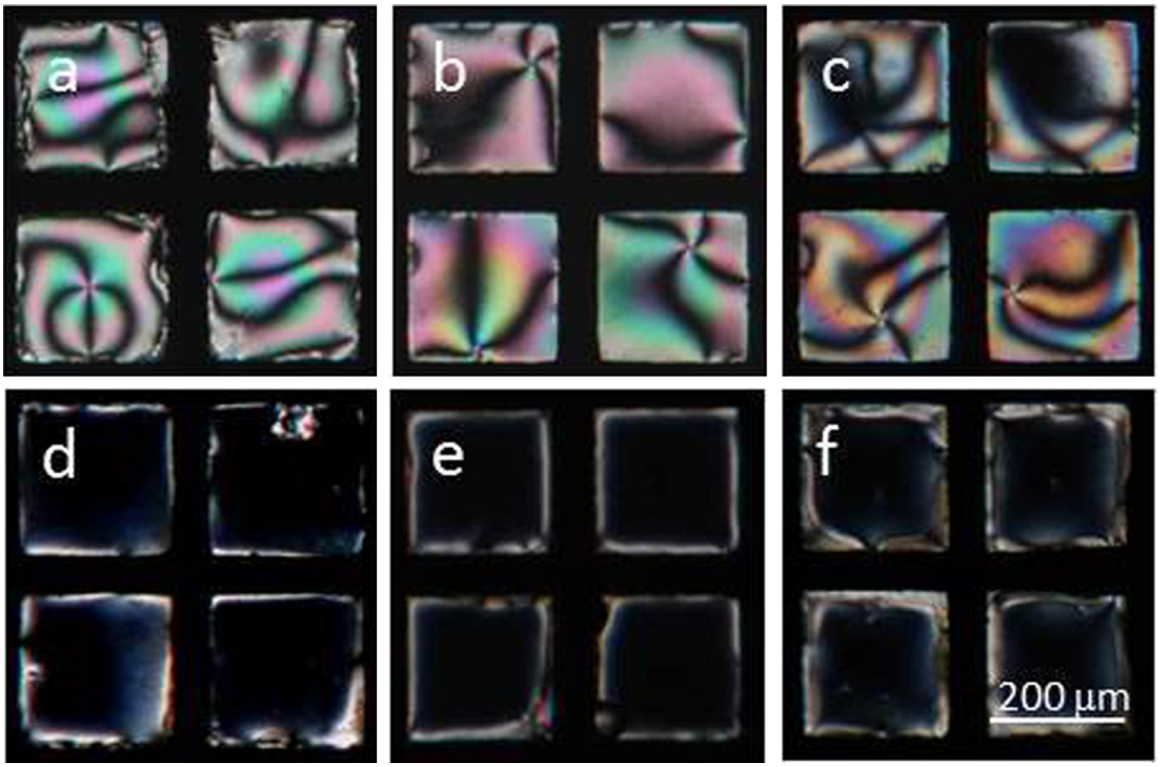

Fig. 4. Polarized image of BSA-modified grids hosting 4′-n-decyloxybiphenyl-4-carboxylic acid doped 5CB immersed in (a) 1 μg/mL, (b) 100 ng/mL, (c) 10 ng/mL, (d) 1 ng/mL, (e) 0.1 ng/mL, (f) 0 ng/mL. The LOD for trypsin is 10 ng/mL.

but there are the same BEs of Au 4f states. The existence of hydrocarbon contamination layer and Au^{+}-thiol ligand induce the negligible blue-shift ($\sim$ 0.1 eV) higher than Au^{0} state of Au foil (84.0 and 87.6 eV) (Chevrier et al., 2012).

Fig. 5e and g exhibit the chemical images of BSA top-layer and gold grid under-layer at C 1s and Au $4f_{7/2}$ state. The results demonstrated that the BSA was hydrolyzed by the trypsin. The intensity line profiles (right panel) reveal that two tendencies on 1st (BSA) and 2nd (trypsin) regions: decreasing height in C 1s state lightly and raising height in Au $4f_{7/2}$ state dramatically. Along C–D line profile, the Au intensity (BE 84.1 eV) in 2nd region is approximately three-times higher than that in 1st region, while C intensity (BE 285.2 eV) shrinks slightly. The C 1s and Au 4f spectra at position 4–6 are displayed in Fig. 5f and h. The similar spectral features before and after trypsin immersion are indicative of that the breaking of peptide bonds in BSA yields the structure compression and reorganization between the parts without the lysine and arginine side chains, but C–C chain is still the majority part of chemical structure of complex molecular species (up to 607 amino acids) (Hu et al., 2012). The fragment loss after trypsin hydrolysis process induced the decrease of carbon signal (i.e. the intensity of XPS at position 6 and line profile around 2nd region). Indeed, the difference of C 1s signal between position 4 and 6 is obscure, yet the change for Au signal is noticeable. This phenomenon can be explained by the fact that fraction of BSA residuals remain on gold grids after the trypsin hydrolysis process was completed. The sampling length of XPS for organic protein molecules is known as 4.5 nm in depth, which is shorter than the reported thickness of BSA layer (4–10 nm by different structural deformations) (Hu et al., 2012; Wu et al., 2006). On the other hand, the photoelectrons generated from the under-layer Au are relatively enhanced by the decreasing thickness and porous structure of the top-layer BSA, which is indicated by the up-raising Au signal around 2nd region. Moreover, BSA is reported to adsorb on the gold surface via the Au–S bond formation using its cysteine side chains (Hu et al., 2012). In our experiments, immersing and washing the BSA-modified gold girds with deionized water cannot break the Au–S bonds, because uniform Au image (measured in SPEM) was found on the samples cleaned by deionized water.

4. Conclusions

We developed the LC-based sensor for trypsin detection by using surface-immobilized BSA as the substrate. Our study showed that when BSA was hydrolyzed by trypsin, the resulting peptide fragments disrupted the orientation of LC at the vicinity, leading to a dark-to-bright transition of the optical image of LC which can be easily distinguished by the naked-eye under ambient light. The LOD of the system for trypsin is approximately 10 ng/mL. In addition, the space and element-resolvable measurements were also deployed to gain an in-depth insight for the detailed responding mechanism between Au, BSA, and trypsin. It was found that the surface density of BSA on the gold grid was significantly reduced after immersing the BSA-modified gold into the trypsin solution, which implies the hydrolysis of BSA by trypsin. This work provides a fundamental principle for designing a LC-based enzymatic assay. By changing the substrates immobilized on the gold grids, one could detect selections of biological interesting targets.

Acknowledgment

We would like to thank Ministry of Science and Technology, Taiwan (MOST 103-2113-M-032-003-MY2, 102-2632-M-032-001-MY3, 104-2112-M-032-005-MY2, and 103-2112-M-032-004) for the funding support.

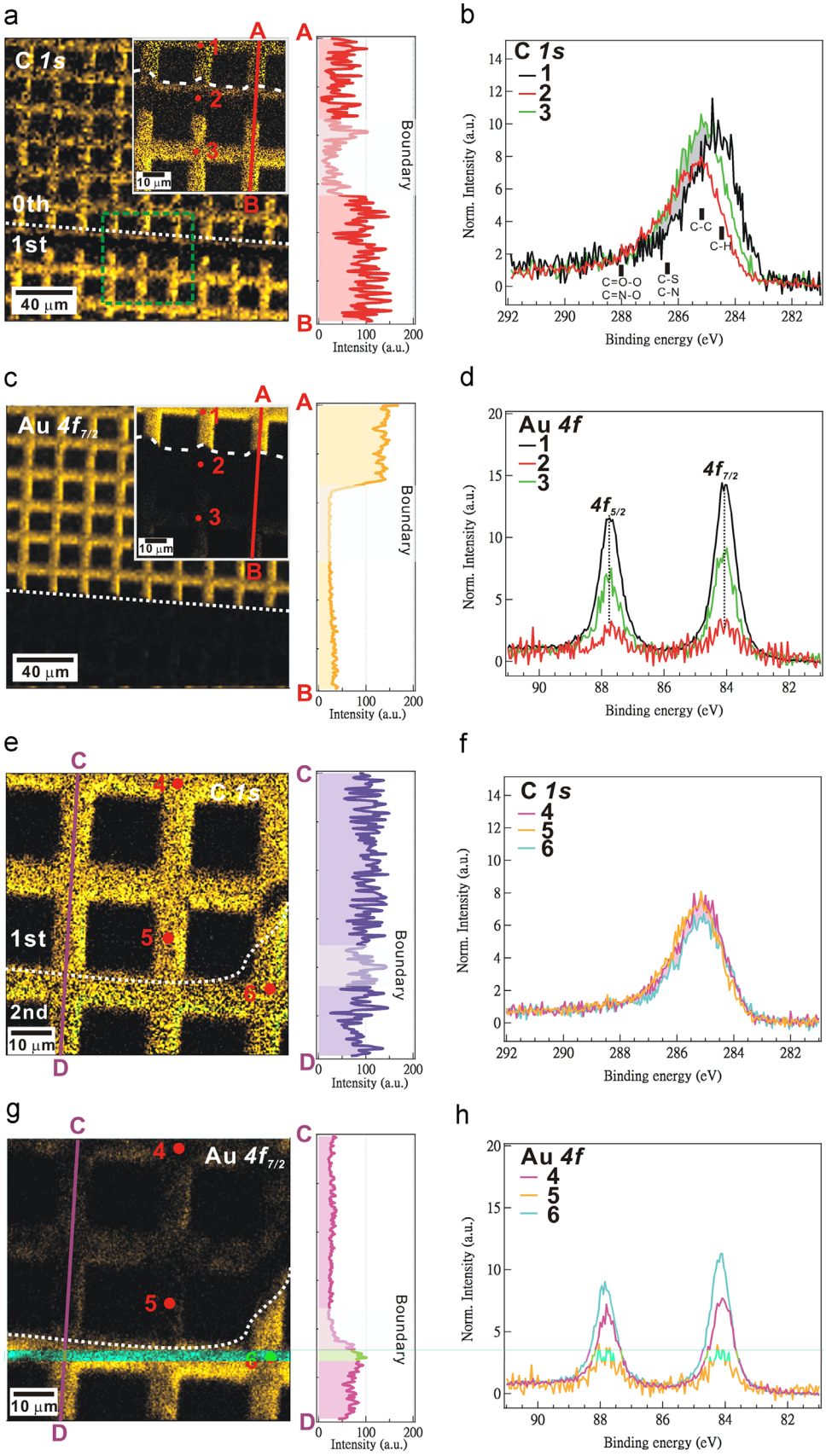

Fig. 5. (a) C 1s and (c) Au 4f images of gold grids (0th) and BSA/Au (1st) area, taken at binding energy of 285.2 and 84.1 eV. The inset plot location is manifested by the green-color square. The right panel is the line profile scheme along A–B line individually from C 1s or Au 4f images. (b)(d) C 1s and (f)(h) Au 4f XPS spectra probed at position 1–6 for the role of BSA adsorption relative to the change of chemical environment. (e) C 1s and (g) Au 4f image varied with the trypsin reaction on BSA protein for the surfaces of BSA/Au (1st) and trypsin/BSA/Au (2nd) sample. (For interpretation of the references to color in this figure legend, the reader is referred to the web version of this article.)

Appendix A. Supplementary material

Supplementary data associated with this article can be found in the online version at http://dx.doi.org/10.1016/j.bios.2015.11.049.

References

Abd-Rabboh, H.S.M., Nevins, S.A., Dürüst, N., Meyerhoff, M.E., 2003. Biosens. Bioelectron. 18, 229–236.
Azioune, A., Siroti, F., Tanguy, J., Jouini, M., Chehimi, M.M., Miksa, B., Slomkowski, S., 2005. Electrochim. Acta 50, 1661–1667.
Bera, T., Fang, J., 2013. Langmuir 29, 387–392.
Bi, X.Y., Hartono, D., Yang, K.L., 2009. Adv. Funct. Mater. 19, 3760–3765.
Brake, J.M., Abbott, N.L., 2002. Langmuir 18, 6101–6109.
Brake, J.M., Daschner, M.K., Luk, Y.Y., Abbott, N.L., 2003. Science 302, 2094–2097.
Chen, C.-H., Lin, Y.-C., Chang, H.-H., Lee, A.S.-Y., 2015. Anal. Chem. 87, 4546–4551.
Chen, C.-H., Yang, K.-L., 2010. Langmuir 26, 1427–1430.
Chen, C.-H., Yang, K.-L., 2013. Sens. Actuators B Chem. 181, 368–374.
Chen, L., Fu, X., Li, J., 2013. Nanoscale 5, 5905–5911.
Chevrier, D.M., Chatt, A., Zhang, P., 2012. J. Nanophotonics 6, 064504.
Chuang, C.H., Chen, C.H., Chang, Y.M., Peng, C.W., Wong, S.S., Tzeng, S.D., Gwo, S., Zhu, Y., Sow, C.H., Lin, M.T., 2007. Appl. Phys. Lett. 91, 183101.
Coco, S., Espinet, P., Marcos, E., 2000. J. Mater. Chem. 10, 1297–1302.
Dong, M., Qi, H., Ding, S., Li, M., 2015. Microchim. Acta 182, 43–49.
Fan, H., Jiang, X., Zhang, T., Jin, Q., 2012. Biosens. Bioelectron. 34, 221–226.
Frateur, I., Lecoeur, J., Zanna, S., Olsson, C.-O.A., Landolt, D., Marcus, P., 2007. Electrochim. Acta 52, 7660–7669.
Gupta, V.K., Skaife, J.J., Dubrovsky, T.B., Abbott, N.L., 1998. Science 279, 2077–2080.
Han, G.R., Song, Y.J., Jang, C.H., 2014. Colloids Surf. B 116, 147–152.
Hu, L., Han, S., Parveen, S., Yuan, Y., Zhang, L., Xu, G., 2012. Biosens. Bioelectron. 32, 297–299.
Hu, Q.Z., Jang, C.H., 2011. Colloids Surf. B 88, 622–626.
Hu, Q.Z., Jang, C.H., 2012. Talanta 99, 36–39.
Hussain, Z., Zafiu, C., Kupcu, S., Pivetta, L., Hollfelder, N., Masutani, A., Kilickiran, P., Sinner, E.K., 2014. Biosens. Bioelectron. 56, 210–216.
Kim, J., Khan, M., Park, S.Y., 2013. ACS Appl. Mater. Interfaces 5, 13135–13139.
Lee, D.-Y., Seo, J.-M., Khan, W., Kornfield, J.A., Kurji, Z., Park, S.-Y., 2010. Soft Matter 6, 1964–1970.
Noone, P.G., Zhou, Z., Silverman, L.M., Jowell, P.S., Knowles, M.R., Cohn, J.A., 2001. Gastroenterology 121, 1310–1319.
Park, J.-S., Teren, S., Tepp, W.H., Beebe, D.J., Johnson, E.A., Abbott, N.L., 2006. Chem. Mater. 18, 6147–6151.
Rubio, C., Costa, D., Bellon-Fontaine, M.N., Relkin, P., Pradier, C.M., Marcus, P., 2002. Colliods Surf. B 24, 193–205.
Sivakumar, S., Wark, K.L., Gupta, J.K., Abbott, N.L., Caruso, F., 2009. Adv. Funct. Mater. 19, 2260–2265.
Suzuki, M., Husimi, Y., Komatsu, H., Suzuki, K., Douglas, K.T., 2008. J. Am. Chem. Soc. 130, 5720–5725.
Wu, Peng, Hogrebe, P., Grainger, D.W., 2006. Biosens. Bioelectron. 21, 1252–1263.
Xue, C.Y., Yang, K.L., 2008. Langmuir 24, 563–567.
Yang, S., Wu, C., Tan, H., Wu, Y., Liao, S., Wu, Z., Shen, G., Yu, R., 2013. Anal. Chem. 85, 14–18.
Yazgan, N.N., Boyaci, S.H., Temur, E., Tamer, U., Topcu, A., 2010. Talanta 82, 631–639.
Zhang, M., Jang, C.H., 2013. Bull. Korean Chem. Soc. 34, 2973–2977.